Supplemental Information: Decoupling First-Cycle Capacity Loss Mechanisms in Sulfide Solid-State Batteries

Emma Kaeli[1,2,*], Zhelong Jiang[1,2], Xiaomian Yang[1], Emma P. K. L. Choy[2,3], Nicolas B. Liang[1,2], Edward Barks[1,2], Sunny Wang[2,3], Stephen D. Kang[1,4,*], and William C. Chueh[1,2,5,*]

[1] *Department of Materials Science and Engineering, Stanford University, Stanford, CA 94305, USA*
[2] *Applied Energy Division, SLAC National Accelerator Laboratory, Menlo Park, CA 94025, USA*
[3] *Department of Chemistry, Stanford University, Stanford, CA 94305, USA*
[4] *Department of Materials Science and Engineering, Seoul National University, Seoul 08826, Republic of Korea*
[5] *Department of Energy Science & Engineering, Stanford University, Stanford, CA 94305, USA*
[*] *Corresponding author.*

1 Data Availability

Data for this Supplemental Information, including the electrochemistry shown here, is available at Harvard Dataverse at `https://doi.org/10.7910/DVN/SGJAVW`.

2 Supplementary Figures

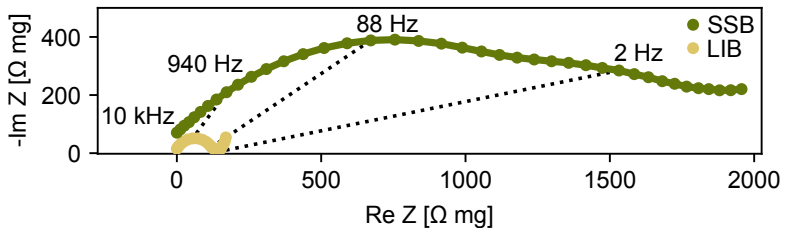

Figure 1: Electrochemical impedance spectroscopy of a SSB and LIB at top of charge (4.3 V) after 10 h voltage hold and 5 minute rest. SSBs exhibit a 10× higher magnitude impedance than the LIB counterpart.

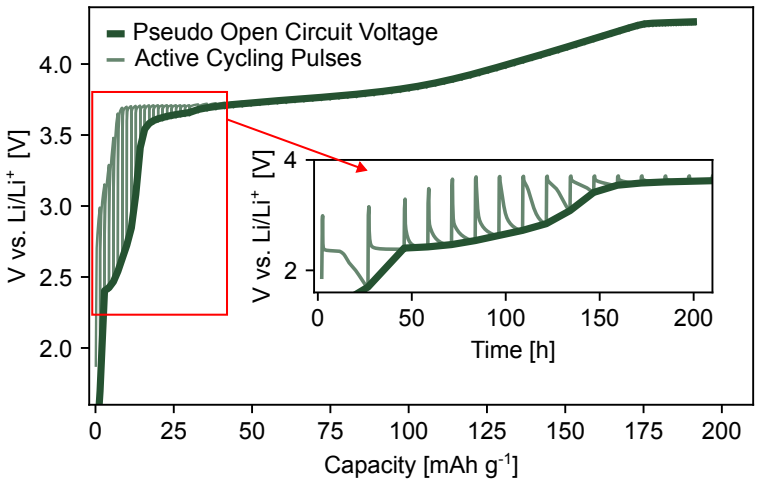

Figure 2: Galvanostatic intermittent titration technique (GITT) used to determine the pseudo-open circuit voltage curve for SSB. Despite using 24 h resting periods, the system did not reach quasi-equilibrium, as evidenced by voltage vs. time decay rates of > 1 mV h^{-1}, particularly in the SE redox region during early cycling. The shoulder extracted from GITT represents 8.9% of first cycle charge capacity, but is an underestimate of total SE oxidation capacity as the cell does not achieve quasi-equilibrium.

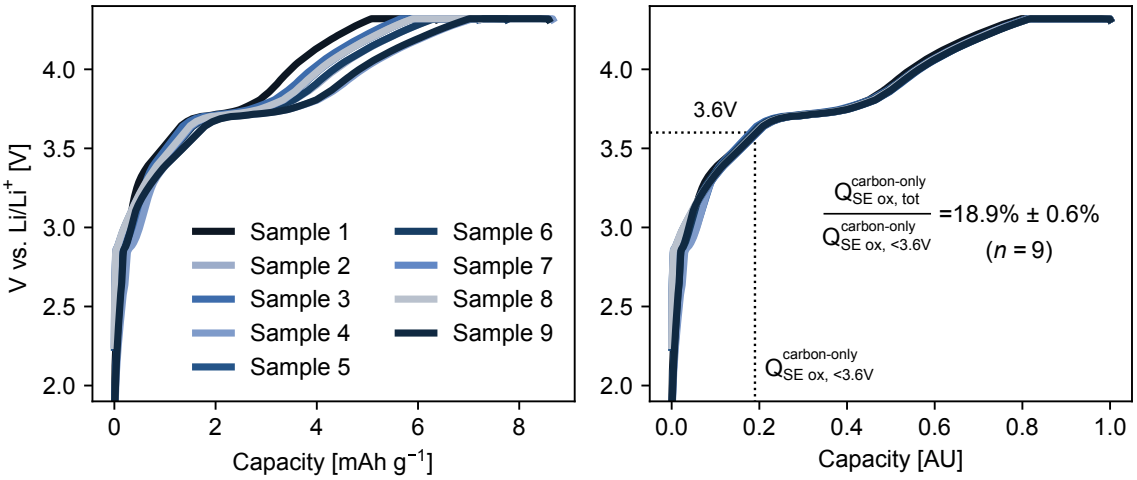

Figure 3: Carbon-only cells cycled with varying amounts of carbon + SE composite added. SE oxidation voltage vs. capacity curves (left) show varied absolute oxidation capacity due to changing carbon + current collector surface area with SE. Voltage vs. capacity curves normalized to SE oxidation capacity (right) demonstrate the ratio of the SE oxidation shoulder capacity to total SE oxidation capacity ($Q^{\text{carbon-only}}_{\text{SE ox, <3.6V}}$ / $Q^{\text{carbon-only}}_{\text{SE ox, tot}}$) yields low variability (mean: 18.9%, standard deviation: 0.6%).

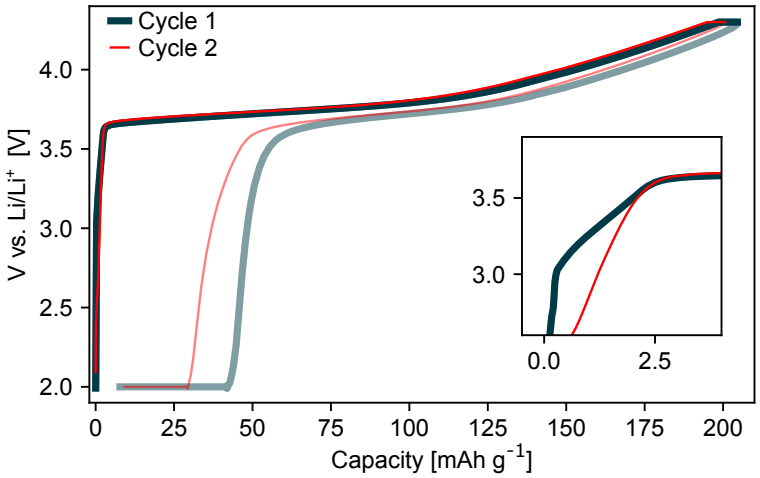

Figure 4: With a long (66 h) voltage hold at 2.0 V, the second cycle is able to recover 96.2% of the first cycle charge capacity, as well as the width of the SE oxidation plateau. The initial (< 1 mAh g^{-1}) shape of the SE oxidation plateau is impacted by In lithiation on first cycle, but the resulting width of the shoulder (2.5 mAh g^{-1}) is similar between first and second cycle.

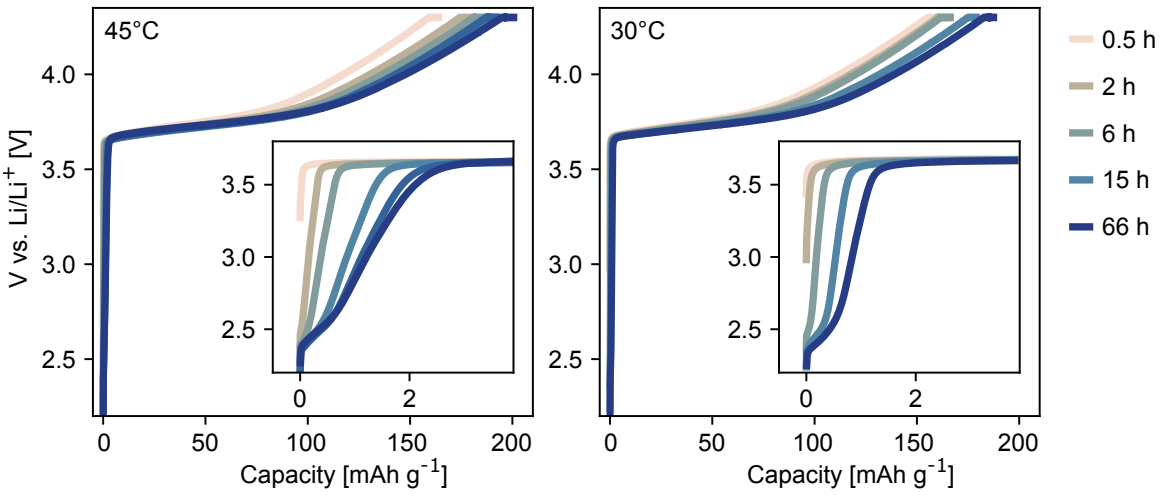

Figure 5: Cycle 2 voltage vs. capacity curves, focused on the shoulder region, after each cell undergoes a 2.0-V discharge hold for varied duration (see legend). Data is shown for cycling performed at 45°C (left) and 30°C (right).

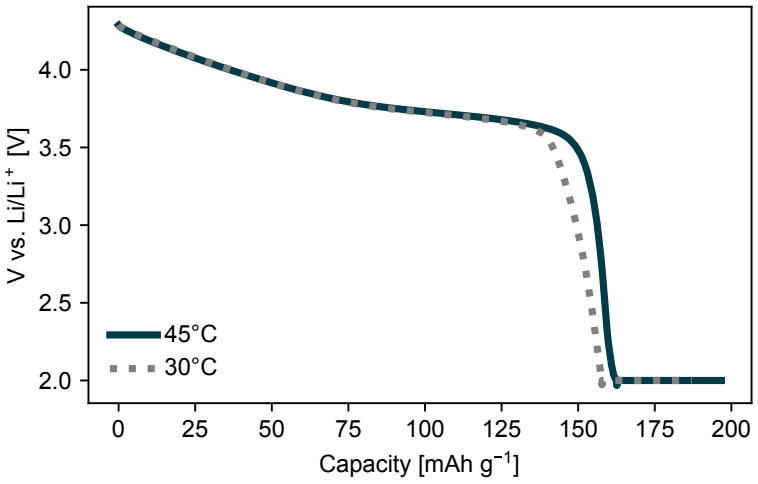

Figure 6: Voltage vs. capacity curves for SSB cells cycled at 45°C and 30°C with 66 h 2.0-V discharge voltage holds. At lower temperatures NMC relithiation kinetics become more sluggish leading to higher overpotentials and reaching the cutoff voltage sooner (at less discharged states) during discharge. We note that the 30°C data is extracted from cycles 0 and 1, and 30°C cycling data is extracted from cycles 4 and 5. See methods for details.

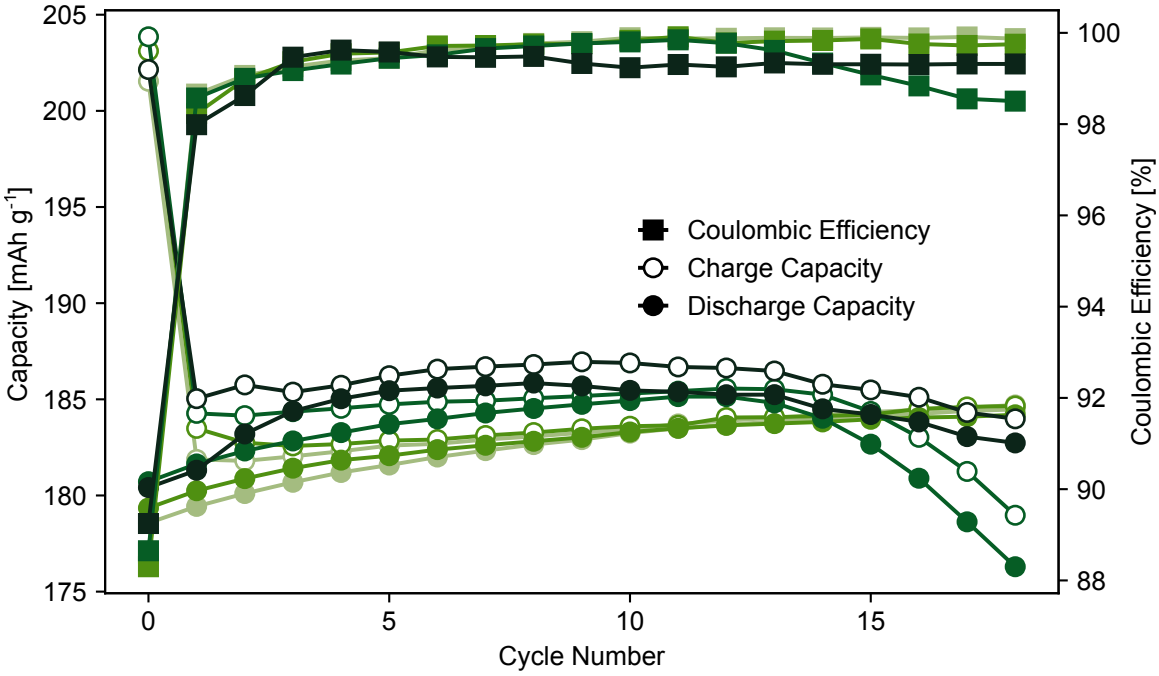

Figure 7: Extended cycling capacity and Coulombic efficiency data for SSBs at 45°C (n=4). We note that toward the end of cycling, SSBs exhibit a decay in discharge capacity, corresponding to accelerated aging phenomena that are exacerbated at higher temperatures.

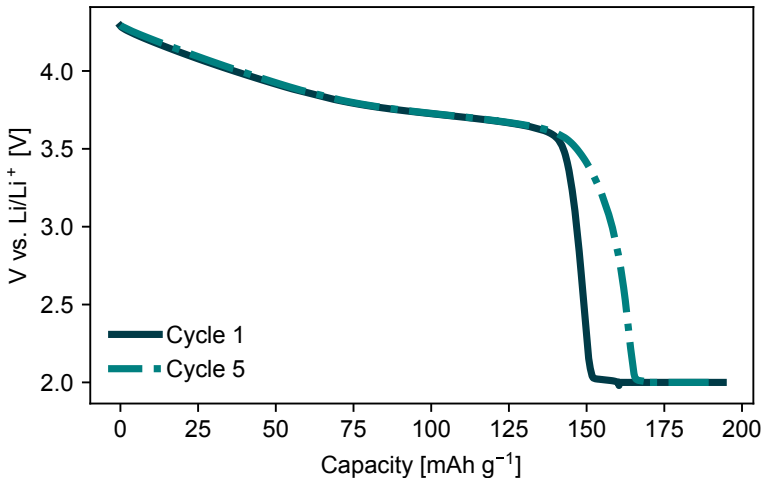

Figure 8: Voltage vs. capacity curves comparing cycle 1 and cycle 5 of SSBs cycled using 33 h 2.0-V discharge voltage hold for every cycle. During later cycles (cycle 5), cells reach the cutoff voltage later (at more discharged states) during discharge than during cycle 1.